

STRUKTURA 2025

Jindřichův Hradec, 8.9.-12.9. 2025

Session I, September 8, Monday

L1

MINERALS WITHIN THE Pd-Ni-As SYSTEM: CRYSTAL STRUCTURES

F. Laufek¹, A. Vymazalová¹, D.A. Chareev², T.L. Grokhovskaya³, V.V. Kozlov³, J. Plášil⁴

¹Czech Geological Survey, Geologická 6, Prague 5, Czech Republic
²Institute of Experimental Mineralogy, RAS, Chernogolovka, Moscow, Russia
³Institute of Geology of Ore Deposits, Petrology, Mineralogy and Geochemistry RAS, Moscow, Russia
⁴Institute of Physics ASCR, v.v.i., Na Slovance 2, 128 21 Prague 8, Czech Republic
frantisek.laufek@geology.cz

There are three ternary phases in the Pd-Ni-As system described as minerals, nipalarsite Ni₈Pd₃As₄, menshikovite Pd₃Ni₂As₃ and majakite, PdNiAs. Majakite and menshikovite were described as new minerals by Genkin [1] and Barkov [2], respectively. Their crystal structures have been hitherto unknown. Nipalarsite was described together with its crystal structure determination by Grokhovskaya et al. [3]. Majakite was found in intergrowths with other platinum minerals in chalcopyrite and thalnakhite ores of the Mayak mine (Talnakh deposit), menshikovite was discovered in mafic-ultramafic layered complexes Lukkulaisvaara and Chiney, Russia. A fragment of menshikovite extracted from a sample from Lukkulaisvaara intrusion, Russia, was used for a structure analysis of this mineral. As the natural majakite proved to be unsuitable for a structural analysis, crystal structure analysis was carried out on a synthetic analogue PdNiAs.

The synthetic analogues of minerals in the system and phases on a Pd₂As-Ni₂As join were prepared using the Kullerud's evacuated silica-glass tube method. Pure elements were used as starting materials for synthesis. The evacuated tube with charges were heated at 400 °C for several weeks. In order to study the extent of the (Pd,Ni) $_2$ As solid solution, selected experiments at the Pd₂As-Ni₂As join were prepared at 450, 500, 520 and 540 °C. The experimental products were rapidly quenched in cold water and analysed by powder or single crystal X-ray diffraction and electron microprobe analysis.

The performed experiments revealed three structurally different phases (solid solutions) along the Pd₂As-Ni₂As join system at 450 °C: -Pd₂As (*Cmc*2₁), -(Pd,Ni) ₂As (*P*-62*m*) and Pd_{1-x}Ni_{1+x}As (*Pnma*). The low-temperature orthorhombic phase -Pd₂As transforms at 484 °C to a hexagonal phase and belongs to the to the high-temperature -(Pd,Ni) ₂As solid solution.

The phase PdNiAs is at 450 °C part of the Pd_{1-x}Ni_{1+x}As solid solution showing *Pnma* symmetry. Its crystal struc-

ture contains a mackinawite-like blocks of edge sharing [NiAs₄] tetrahedra parallel to (001). Palladium shows unusual five-fold coordination resembling a tetragonal pyramid by As atoms. The coordination of Pd is further completed by close contacts with Ni and Pd atoms. Palladium atoms are located in voids between blocks of [NiAs₄] tetrahedra. A phase transition from low-temperature orthorhombic phase to the high-temperature hexagonal phase was observed. The hexagonal phase PdNiAs was also described by Evstigneeva [4]. Menshikovite Pd₃Ni₂As₃ crystal structure contains deformed [NiAs₄] tetrahedra. Each [NiAs₄] tetrahedra shares one edge with one adjacent tetrahedra along the a-axis and two opposing edges with adjacent tetrahedra along the c-axis forming chains of edge-shared [NiAs₄] tetrahedra running in 001 direction. Nickel atoms have three close contacts with adjacent Ni atoms across the shared tetrahedral edges. Palladium atoms show trigonal bipyramidal coordination by As atoms.

- A. D. Genkin, T.L. Evstigneeva, N.V. Troneva, L.N. Valsov, *Int. Geol. Rev.*, 20, (1976), 96.
- A. Y. Barkov, R.F. Martin, Y.A. Pakhomovsky, N.D. Tolstykh, A.P. Krivenko, *Can Mineral.*, 40, (2002), 679.
- T. L. Grokhovskaya, O.V. Karimova, A. Vymazalová, F. Laufek, D.A. Chaarev, E.V. Kovalchuk, L.O. Magazina, V. A. Rassulov. *Min. Mag.*, 83, (2019), 837.
- 4. T. Evstigneeva, Y. Kabalov, J. Schneider. Material Science Forum, 321-324, (2000), 700.

This research was supported by the by the Strategic Research Plan of the Czech Geological Survey (DKRVO/ČGS 2023–2027).



PHASE ANALYSIS OF SOIL SEDIMENTS WITH REGARD TO THE PRESENCE OF ASBESTOS MINERALS

Zdeněk Jansa, Štěpánka Jansová, Ján Minár

New Technologies Research Centre, University of West Bohemia in Pilsen, Pilsen

The aim of this work is to summarize current knowledge on the extensive issue of asbestos occurrence in general and in the Pilsen Region of the Czech Republic, to establish a suitable methodology for detecting the presence of naturally occurring asbestos in soil deposits in a given location based on experimental analyses motivated by analyses in other countries, and to accurately identify individual types of asbestos from a series of samples. Twelve samples were evaluated as part of this work, and this paper presents a summary of them. [1, 2]

The morphology and elemental composition of the studied samples were evaluated using scanning electron microscopy with an energy dispersive spectrum detector. Figure 1 shows examples of fibers resembling needles with very sharp ends, which morphologically corresponded to the amphibole group, and long, wavy fibers, which corresponded to the serpentine group.

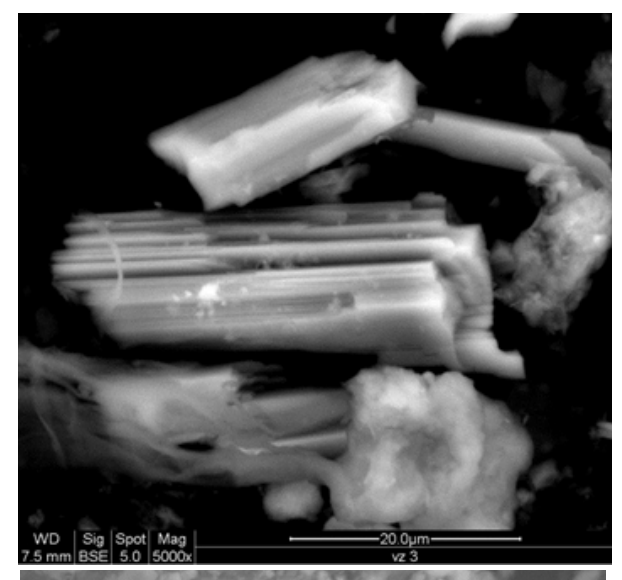
The basic building block of the silicate structure of asbestos is the silicon-oxygen tetrahedron $[SiO_4]^{4-}$. Chrysotile, as a representative of the first group of asbestos serpentines, is hydrated magnesium silicate and its stoichiometric chemical composition can be given as $Mg_3Si_2O_5(OH)_4$. However, it has been observed that the chemical composition of the fibrous phase is closely related to the composition of the surrounding rock matrix and can be highly variable, as can be seen in the overview of the summary formulas of asbestos compounds in Table 1. [3, 4, 5]

The chemical composition of minerals that make up the second group of asbestos—amphiboles—reflects the complexity of the environment in which they were formed and can vary considerably in terms of major and trace elements and other influences that contributed to their formation. Amphibole fibers can be considered a series of minerals in which one cation is gradually replaced by another. [6, 7]

The second method used was X-ray phase analysis. The samples were measured under identical conditions. The measurements were performed on a Panalytical X'Pert Pro powder diffractometer with a copper X-ray tube (K $_{\rm 1}$ = 0.154 nm). An ultra-fast Pixcel semiconductor detector was used with evaluation in the High Score program. Standard symmetrical geometry with a Bragg-Brentano arrangement was used for the measurements.

The measurement range for all samples was set identically between 20 and 85° [2]. When evaluating the samples, it was found that the main diffraction lines are located within an angle of 40° [2], while other diffraction lines beyond this angle belong to the ${\rm SiO_2}$ phase. Therefore, a section ranging from 20° to a maximum of 40° [2] was selected on all diffractograms.

Figure 2 shows the diffraction patterns of samples 1 and 2, before and after annealing, with the identified phases



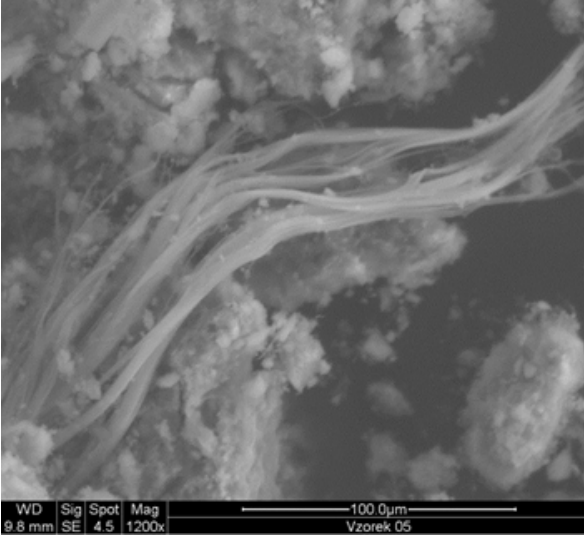


Figure 1. Images of samples 3 and 5.

marked in the range from 20 to a maximum of $40^{\circ}[2]$. The numerical designation of these phases corresponds to the numerical designation of the identified phases in Table 2.

Since the evaluation of the diffraction patterns of the unprocessed samples revealed a significant presence of organic components in the samples, all samples were annealed before further measurement. The samples were annealed at 530 °C for 4 hours and then cooled naturally. The temperature of 530 °C is below the thermal decomposition temperature of asbestiform minerals, so there was no loss of native information from the samples.

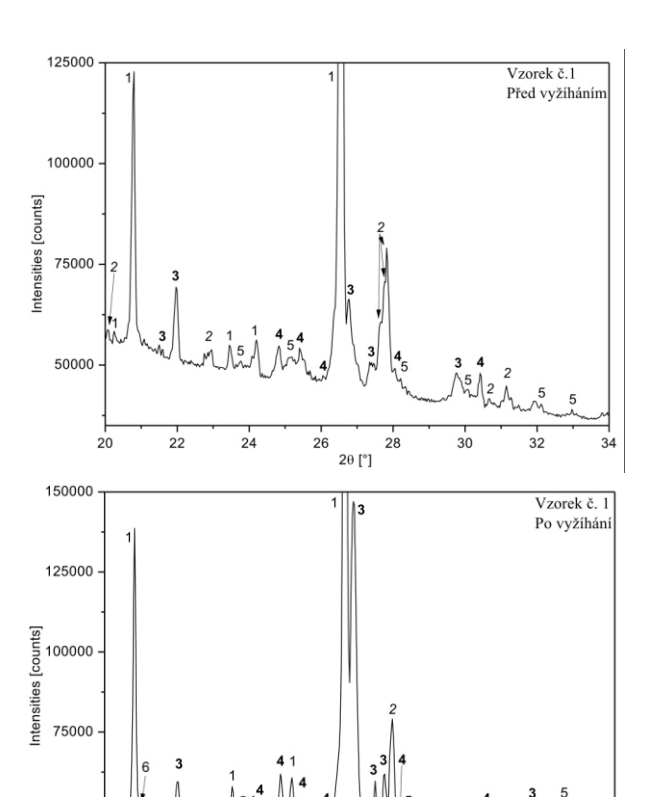
Scanning electron microscopy confirmed the presence of fibers that, from a morphological point of view, corre-



50000

Table 1. Summarized formulas of asbestos compounds.

Chrysotile	$Mg_2Si_2O_5(OH)_4$
Amosite	Mg ₃ Si ₂ O ₅ (OH) ₄ (Fe ₂ , Mg) ₇ Si ₈ O ₂₂ (OH) ₂
Crocidolite	Na ₂ (Fe Mg) Fe ² Si O 2(OH) ₂ (Mg, Fe ₂) Si O 2(OH) ₂ (Mg, Fe ₂) Si O 22(OH) ₂
Antophylite	$(M_g^2, F_{e_3}^2)_7 Si_8^3 O_{22}^2 (OH)_2^2$
Tremolite	$Ca_2Mg_5Si_9O_{22}(OH)_2$
Aktinolite	$\text{Ca}_{2}^{2}(\text{Mg}, \text{Fe}_{2}^{2})_{5}^{2}\text{Si}_{8}\text{O}_{22}^{2}(\text{OH})_{2}$



Figures 2. Evaluated diffractograms of sample 1 and 2 with identification of phases.

sponded to both main groups of asbestos minerals, namely the serpentine and amphibole groups. X-ray diffraction identified individual phases in the samples and determined the exact type of asbestos minerals found.

Table 2. Table of identified phases in soil sediment samples.

No	Mineral	Name of compound	Reference code	Chemical formula
1	quartz	silicon oxide	01-089-8935	SiO ₂
2		magnesium silicate	01-086-0433	Mg ₂ (Si ₂ O ₆)
3	antofylit	antofylite	96-901-6382	Mg ₂₈ Si ₃₂ O ₉₆
4	chryzotil	chryzotile	96-101-0961	Si ₁₆ Mg ₂₄ O ₇₂
5	wollastonit	calcium silicate	01-072-2297	CaSiO ₃
6		hydrogen silicate	00-031-0581	H ₂ Si ₂ O ₅

Table 3. Summary table of identified asbestos types

Sample ID	Chrysotile	Anthophyllite	Actinolite
S1:sample 1-2	X	X	X
S1:sample 3-4	X	X	X
S2:sample 1'-8'	X	x (except 6')	X

After compiling the data from all analyses, we can say with certainty that chrysotile from the serpentine group is present in all evaluated samples. This is the least dangerous form of asbestos. Furthermore, we can say that the presence of anthophyllite from the amphibole group has been confirmed in all samples. Based on the morphology of the fibers, it is highly likely that crocidolite is also present in one sample, but this has not been confirmed by X-ray diffraction. The results of the asbestos found are shown in Table 3.

The combination of SEM analysis and X-ray diffraction provides a good set of tools for identifying asbestos. By gradually refining the measured diffraction pattern of the sample under investigation, it is possible to accurately determine the phases present, despite the complexity of the process.

- F. Skácel, Z. Guschlová a V. Tekáč: Azbestová a minerální vlákna ve vnitřním ovzduší, Ústav plynárenství, koksochemie a ochrany ovzduší VŠCHT v Praze, Chemické listy 106, 961-970, 201.
- Lajčíková, M. Hornychová: Azbest v ovzduší a legislativní zajištění ochrany zdraví, Státní zdravotní ústav Praha, 55(3), 99-101, 2010.
- M. Novák: Mineralogický systém, prezentace [online cit. 2021-12-06], Masarykova univerzita, available from: https://is.muni.cz/el/sci/podzim2011/G1061/Minera-I-syste m3a.pdf.
- C. E. Housecroft, A. G. Sharpe: Anorganická chemie, ISBN 978-80-7080-872-6.
- U.S. DEPARTMENT OF THE INTERIOR U.S. GEOLOGICAL SURVEY Asbestos: Geology, Mineralogy, Mining, and Uses by Robert L. Virta1, Open-File Report 02-149.
- O.C. Wells: Scanning Electron Microscopy, McGraw-Hill, New York (1974).

7. M.Kužvart, Z. Weiss, Jílové materiály, jejich nanostruktura a využití, Praha červen 2005, ISBN 80-246-0868-5



PROPERTIES OF SCHWERTMANNITE: THE CRITICAL ROLE OF PHASE PURITY

C. Pilloni¹, V. Mameli^{2*}, T. Kmječ³, V. Gajdošova⁴, C. Cannas², D. Zákutná^{1*}

Department of Inorganic Chemistry, Charles University, Hlavova 2030, Prague 2 128 40, Czech Republic Department of Chemical and Geological Sciences, University of Cagliari, Cittadella Universitaria S.P. Monserrato Sestu Km 0.700, 09042 Monserrato, Italy

³Department of Low-Temperature Physics, Faculty of Mathematics and Physics, Charles University, V Holešovičkách 2, 180 00 Prague, Czech Republic

⁴Institute of Macromolecular Chemistry, Academy of Sciences of the Czech Republic, 162 06 Prague 6, Czech Republic

valentina.mameli@unica.it, zakutnad@ill.fr

Schwertmannite, a poorly crystalline iron oxyhydroxysulphate, is an iron-bearing mineral that plays a pivotal role in various environmental processes, particularly in the treatment of acidic mine drainage [1]. Due to its ability to adsorb metal ions, anions, and its high surface area-to-volume ratio, schwertmannite has drawn significant attention as a potential medium for mitigating environmental contamination [2]. However, its poorly crystalline structure presents significant challenges in characterising its composition, making it difficult to detect and to quantify trace impurities. One such impurity is goethite, another iron mineral that can form under similar conditions due to higher thermodynamic stability [3]. Differentiating between schwertmannite and goethite in environmental or

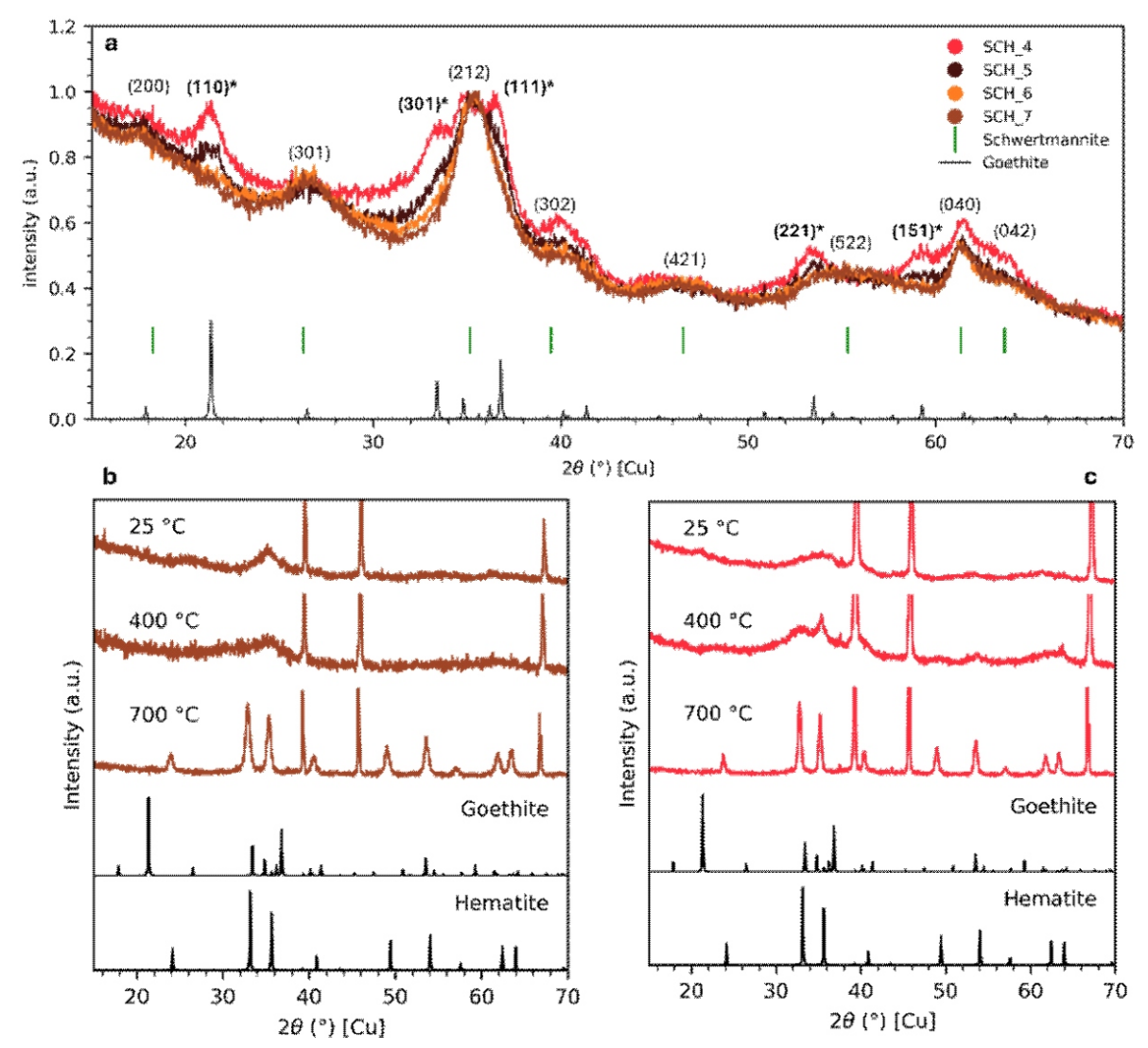


Figure 1. a) room temperature powder x-ray diffraction pattern of all the samples, high-temperature powder x-ray diffraction pattern of: b) SCH4, sample richer in goethite, and c) SCH7, purest sample.



synthetic samples is crucial, as the presence of goethite affects the chemical reactivity and stability of schwertmannite, thereby altering its efficiency in ecological applications. The aim of this study is to characterise four synthetic samples of schwertmannite with different levels of goethite impurity. The presence was detected using a combination of Room-Temperature Powder X-ray Diffraction (RT-PXRD) and High-Temperature Powder X-ray Diffraction (HT-PXRD), Fourier Transform Infrared spectroscopy in Attenuated Total Reflectance mode (ATR-FTIR), and Thermogravimetric Analysis (TGA), with characteristic features in all the techniques. Notably, increasing precursor concentration led to decreased goethite content in the samples, as evidenced by the progressive disappearance of diffraction maxima observed from RT-PXRD (Fig. 1a). This is further confirmed by the presence of the hematite diffraction maxima after 400 °C in the samples richer in goethite (Fig. 1b, c). Interestingly, only magnetisation measurements provide information on the presence of goethite in the purest sample, demonstrating it as a powerful probe for this poorly crystalline system. These findings confirm that magnetic characterization based on Vibrating Sample Magnetometer (VSM) can serve as an effective tool for identifying goethite impurities in schwertmannite, thereby contributing to the knowledge of poorly crystalline iron materials, and highlighting the potential of magnetic techniques for enhancing our comprehension of these materials in both natural and engineered systems.

- J. M. Bigham, U. Schwertmann, S. J. Traina, R. L. Winland, and M. Wolf, 'Schwertmannite and the chemical modeling of iron in acid sulfate waters', *Geochim. Cosmochim. Acta*, vol. 60, no. 12, pp. 2111–2121, Jun. 1996, doi: 10.1016/0016-7037(96)00091-9.
- B. Marouane *et al.*, 'The potential of granulated schwertmannite adsorbents to remove oxyanions (SeO32-, SeO42-, MoO42-, PO43-, Sb(OH)6-) from contaminated water', *J. Geochem. Explor.*, vol. 223, p. 106708, Apr. 2021, doi: 10.1016/j.gexplo.2020.106708.
- 3. P. Acero, C. Ayora, C. Torrentó, and J.-M. Nieto, 'The behavior of trace elements during schwertmannite precipitation and subsequent transformation into goethite and jarosite', *Geochim. Cosmochim. Acta*, vol. 70, no. 16, pp. 4130–4139, Aug. 2006, doi: 10.1016/j.gca.2006.06.1367.



IMPROVING THERMOELECTRIC EFFICIENCY OF MULTILAYER ScN/Sc_{1-x}Nb_xN HETEROSTRUCTURES BY Nb DOPING

Joris More-Chevalier¹, Urszula. D. Wdowik², Jiří Martan³, Xavier Portier⁴, Stanislav Cichoň¹, Esther de Prado¹, Petr Levinský¹, Ladislav Fekete¹, Jan Pokorný¹, Dejan Prokop^{1,5}, Petr Hruška^{1,5}, Markéta Jarošová¹, Jan Kejzlar¹, Dominik Legut^{2,5}, Michal Novotný¹, Ján Lančok¹

¹Institute of Physics of the Czech Academy of Sciences, Na Slovance 2, 18221 Praha 8, Czech Republic ²IT4Innovations, VSB - Technical University of Ostrava, 17. listopadu 2172/15, CZ 708 00 Ostrava-Poruba, Czech Republic

³New Technologies Research Centre (NTC), University of West Bohemia, Univerzitni 8, 301 00 Plzeň, Czech Republic

⁴CIMAP Normandie Université, ENSICAEN, UNICAEN, CEA, UMR CNRS 6252, 6 Boulevard Maréchal Juin, 14050 Caen Cedex 4, France

⁵Faculty of Mathematics and Physics, Charles University, Ke Karlovu 3, 121 16 Prague 2, Czech Republic

The thermoelectric properties of $ScN/Sc_{1-x}Nb_xN$ multilayers deposited on MgO (001) substrates were investigated using a combined experimental and theoretical approach based on the density functional theory. Four multilayers were prepared, exhibiting total Nb percentages of 0.4 %, 1.2 %, 1.8 %, and 4.8 % atomic ratio in the samples. Structural characterization confirmed the epitaxial

growth of multilayers with sharp interfaces. Thermoelectric measurements showed an enhancement of the Seebeck coefficient and a reduction in thermal conductivity with Nb-doped ScN interlayers. The figure of merit (ZT) was potentially increased to over 0.3. This improvement highlights the promise of this approach for enhancing the thermoelectric performance of scandium nitride.

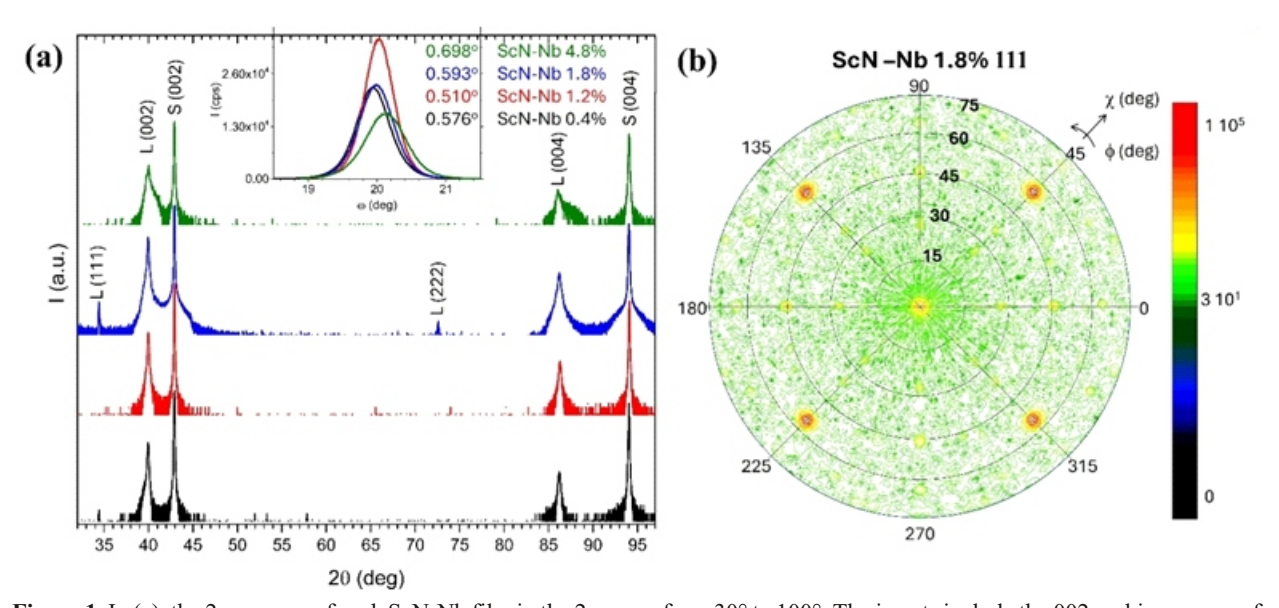


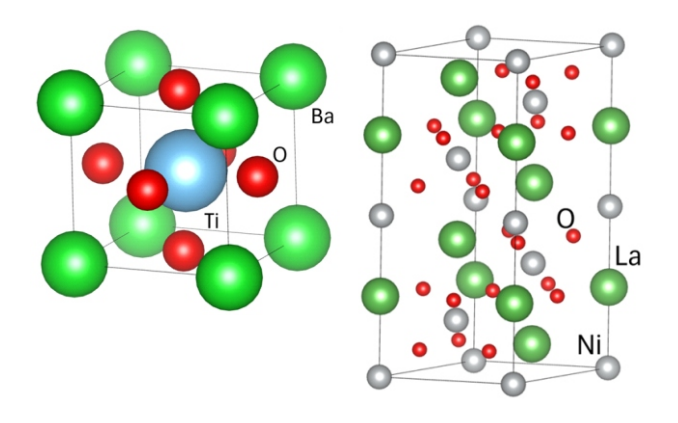
Figure 1. In (a), the 2 scans of each ScN-Nb film in the 2 range from 30° to 100°. The inserts include the 002 rocking curves of each film, including the FWHM, which are equal to 0.576°, 0.510°, 0.593°, and 0.698° for the multilayer films containing 0.4%, 1.2%, 1.8%, and 4.8% of Nb, respectively. In (b), 111 pole figure of the ScN-Nb 1.8%.



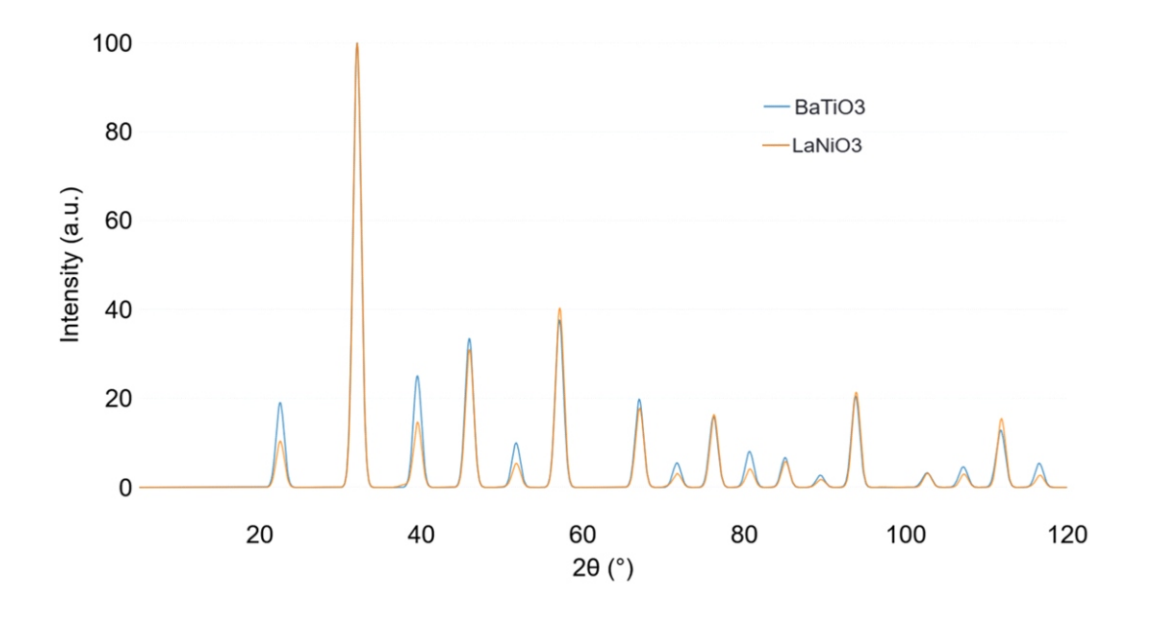
TENKÉ VRSTVY BaTiO₃/LaNiO₃: OD DIFRAKCE K POČÍTAČOVÝM SIMULACÍM J. Drahokoupil^{1,2,3}, M. Lebeda^{1,2,3}, J. Remsa¹

¹Fyzikální ústav, Akademie věd České Republiky, Na Slovance 2, 182 21 Praha 8, Česká Republika
²Katedra inženýrství pevných látek, Fakulta jaderná a fyzikálně inženýrská v Praze, České vysoké učení technické v Praze, Technická 4, 166 07 Praha 6 - Dejvice, Česká Republika
³Ústav fyziky, Fakulta strojní, České vysoké učení technické v Praze, Technická 4, 166 07 Praha 6 - Dejvice, Česká Republika
Česká Republika
draho@fzu.cz

Barium titanát, BaTiO₃ (BTO) je klíčový materiál v moderní elektronice, kde má velmi široké uplatnění díky svým feroelektrickým, dielektrickým a piezoelektrickým vlastnostem. Další zajímavou látkou je LaNiO3 (LNO), který je jako jeden z mála perovskitů vodivý i při pokojové teplotě, a proto nachází uplatnění např. v tenkých vrstvách v kombinaci s ostaními perovskitovými materiály. Tento příspěvek se bude věnovat charakterizaci a teoretickým předpovědím směsného perovskitu BTO/LNO, který byl připraven ve formě tenkých vrstev na křemíkovém substrátu. Pro přípravu těchto vrstev byl použit unikátní systém skládající se s klasického PLD (pulzní laserová depozice) systému obohaceného o druhý terč v tzv. "off-axis" poloze. Snaha o přípravu objemových vzorků vede většinou ke vzniku více fází. Ač se na první pohled tyto dva krystalické systémy líší, viz obr. 1 – BTO bývá při pokojové teplotě v pseuduokubické struktuře s malou tetragonální výchylkou a LNO má při pokojové teplotě rhobohedrickou strukturu jsou difrakční záznamy těchto dvou perovskitů podobné. Při vhodné volbě mřížových parametrů dokonce těžko rozlišitelné – viz obr. 2.



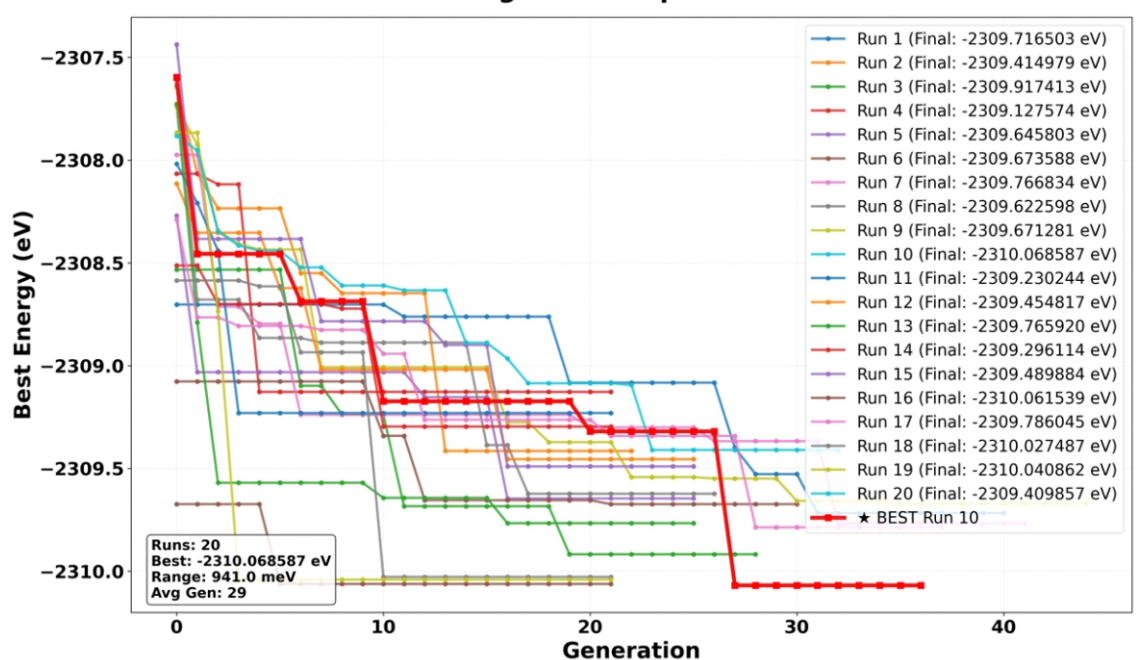
Obrázek 1. Krystalová struktura BaTiO₃ (vlevo) a LaNiO₃ (vpravo).



Obrázek 2. Teoretické difrakční záznamy pro BaTiO₃ (P4*mm* - *a* = 3,943, *b* = 3,958) a LaNiO₃ (R-3cH - a = 5,578, c = 13,677). (Nagenerováno pomocí programu XRDlicious)



GA Convergence Comparison - All Runs



Obrázek 3. Několik běhů genetického algoritmu s cílem najít energeticky nejvýhodnější obsazení atomových pozic – výstup z programu MACE GUI.

Připravené vrstvy s různou koncentrací BTO či LNO vykazují krystalickou formu a difrakční záznam ukazuje, v rámci svého rozlišení, na jednu krystalickou mřížku. Vzhledem k pozorovanému rozšíření dikrakčních píků rozlišit nelze velmi podobné mřížky rozlišit a nelze vyloučit separaci na části bohatší na Ba resp. La.

Kromě různých experimentální technik byl tento systém studováni také pomocí DFT výpočtů a pomocí strojově naučeného (na DFT data) meziatomové potenciálu MACE a jeho implementaci do námi vytvořeného (nejenom) grafického rozhraní MACE GUI. Kromě výpočtu mřížkových parametrů jsme se zajímali i o energetickou výhodnost obsazovaní konkrétních atomových pozice různými prvky.

Na obr. 3 je zobrazeno několik běhů genetického algoritmu s cílem najít vhodné rozmístění Ba/La a Ti/Ni v superbuňce obsahující 320 atomů. Superbuňka vycházela z tetragonální struktury BTO a předpokládali jsme, že La obsazuje stejnou atomovou pozici jako Ba a Ni stejnou atomovou pozici jako Ti. Mřížkové parametry pro studovanou koncentraci 50:50 byli převzaté z experimentální dat a geometrická optimalizace pozic atomů či velikosti superbuňky nebyla prováděna. Je patrné, že pro takto velkou superbuňku nebylo velmi pravděpodobně nalezeno globální minimum, protože každý běh dopadl jinak.



Session II, September 8, Monday

L6

LIGHT INDUCED HALIDE SEGREGATION IN MIXED-HALIDE PEROVSKITES

P. Machovec¹, L. Horák¹, M. Dopita¹, V. Holý^{1,2}

¹Faculty of Mathematics and Physics, Charles University, Ke Karlovu 5, 121 16 Prague 2, Czech Republic, ²Institute of Condensed Matter Physics, Masaryk University, Kotlářská 2, 611 37 Brno, Czech Republic, petr.machovec@matfyz.cuni.cz

Mixed-halide perovskites (MHPs) exhibit tunable band gaps, making them attractive for tandem photovoltaic applications. However, under illumination, halide ions migrate and segregate into iodine- and bromine-rich regions, reducing device efficiency. Here, we present a quantitative X-ray diffraction (XRD) approach for resolving the spatial distribution of halide ions during and after illumination. We present a model linking local composition fluctuations to strain fields, atom displacements, and diffuse scattering, enabling fitting of measured diffraction profiles from polycrystalline $FA_{0.83}Cs_{0.17}Pb(I_{0.6}Br_{0.4})_3$ thin films and $FA_{0.83}Cs_{0.17}Pb(I_{0.85}Br_{0.15})_3$ single crystals.

Illumination experiments were conducted using a solar simulator at 1 Sun equivalent, with diffraction patterns measured before and after 10 min and 30 min light exposures, followed by relaxation in darkness for up to two days. The concentration of Br within the sample was modelled by a random function with a correlation function

exp
$$\frac{|\vec{r} \cdot \vec{r}'|}{2}$$
 and the experimental data were fitted us-

ing model of X-ray scattering, with parameters including the root mean square (rms) Br concentration deviation , correlation length $\,$ grain radius $\,$ R, and asymmetry factor

In pristine polycrystalline samples, diffraction peaks were symmetric, consistent with a cubic perovskite lattice with mean grain radius of 50 nm. Illumination induced asymmetric broadening toward higher diffraction angles, increasing with scattering angle, and accompanied by

slight peak shifts to lower 2 . The fits revealed a significant rise in during illumination, indicating enhanced fluctuations in local composition, followed by slow partial relaxation in darkness within tens of hours. The asymmetry factor á remained consistently > 5, which is the limit of sensitivity of our model to this parameter, indicating the formation of highly bromide-rich regions embedded in a slightly iodine-rich matrix—an observation not previously observed by optical probes such as photoluminescence, which reported I-rich domains. The correlation length was found to be 15 nm and unaffected by illumination cycles.

For the single crystal samples reciprocal space maps were measured before and after 30 minutes of light soaking. We attempted fitting the data with the same correlation function as the polycrystalline samples, but the shape of the diffraction maxima can't be properly fitted. A distribution of the Br concentration consisting of Br-rich spheres in slightly I-rich volume was used to achieve good fit.

The results suggest that illumination drives preferential outward migration of Γ ions from nucleation sites such as grain boundaries or defects, leading to the observed microstructure. The method provides quantitative, bulk-sensitive insight into light-induced halide segregation, complementing surface-sensitive optical techniques. It also highlights the incomplete reversibility of segregation. This quantitative diffraction-based approach offers a new pathway to investigate ionic migration and microstructural evolution in perovskite optoelectronic materials.





THIOPHENE-BASED CONDUCTIVE POLYMERS: STRUCTURAL ORDER VS. CONDUCTIVITY

Dominik Farka

Faculty of Science, University of South Bohemia in České Budějovice, Czech Republic farka@prf.jcu.cz

Polythiophenes dominate the field of conductive polymers. This is in particularly true for the renowned PEDOT, where particularly outstanding charge-transport properties were observed. In this talk, three, state-of-the-art conductive polymers synthesized via tube-furnace oxidative chemical vapour deposition (oCVD) are presented. We will focus on the role of substitution-effects, the role of the counter-ion in achieving large crystallites in thin-films and related charge transport. Alternative emerging methods will be discussed in terms of an outlook.

- Farka, D.; Coskun, H.; Gasiorowski, J.; Cobet, C.; Hingerl, K.; Uiberlacker, L. M.; Hild, S.; Greunz, T.; Stifter, D.; Sariciftci, N. S.; Menon, R.; Schoefberger, W.; Mardare, C. C.; Hassel, A. W.; Schwarzinger, C.; Scharber, M. C.; Stadler, P. Anderson-Localization and the Mott-Ioffe-Regel Limit in Glassy-Metallic PEDOT. AEM 2017, 3 (7), 1700050.
- 2. Farka, D.; Greunz, T.; Yumusak, C.; Cobet, C.; Mardare, C. C.; Stifter, D.; Hassel, A. W.; Scharber, M. C.; Sariciftci,

- N. S. Overcoming Intra-Molecular Repulsions in PEDTT by Sulphate Counter-Ion. Science and Technology of Advanced Materials **2021**, 22 (1), 985–997. https://doi.org/10.1080/14686996.2021.1961311.
- Farka, D.; Kříž, K.; Fanfrlík, J. Strategies for the Design of PEDOT Analogues Unraveled: The Use of Chalcogen Bonds and -Holes. J. Phys. Chem. A 2023, 127 (17), 3779–3787. https://doi.org/10.1021/acs.jpca.2c08965.
- Farka, D.; Moreda, O. I.; Greunz, T.; Kříž, K.; Leeb, E.; Ulbricht, C.; Duchoslav, J.; Vacek, J.; Fanfrlík, J.; Yumusak, C.; Drnec, J.; Krajcovic, J.; Stifter, D.; Sariciftci, N. S. Polythieno[3,4-b]Pyrazine: Pathways to Metallic Charge-Transport. J. Mater. Chem. A 2025. https://doi.org/10.1039/d5ta01145k.
- Farka, D.; Ciganek, M.; Veselý, D.; Kalina, L.; Krajčovič, J. Epitaxial Guidance of Adamantyl-Substituted Polythiophenes by Self-Assembled Monolayers. ACS Omega 2024, 9, 38733–38742. https://doi.org/10.1021/acsomega.4c04616.

L8

POLYMORPHS OF Zn_xCu_{4-x}(OH)₆Cl₂ AND THEIR PHYSICAL PROPERTIES P. Doležal^{1,2}, V. Starosta¹, C. Krellner³, P. Puphal⁴, A. Pustogow²

¹Department of Condensed Matter Physics, Charles University, Czech Republic
²Institute of Solid State Physics, TU Wien, Austria
³Physikalisches Institut, Goethe-Universität Frankfurt, Germany
⁴Max Planck Institute for Solid State Research, Stuttgart, Germany
petr.dolezal@matfyz.cuni.cz

Quantum spin liquid (QSL) is a theoretical model of spins with antiferromagnetic interactions. These spins fluctuate down to the absolute zero temperature without any long-range magnetic order but exhibit quantum entanglement [1]. A key aspect for realization of such theoretical concept is a geometrical frustration of these spins. In theory various OSL states have been identified, but much harder is to find a material, where this concept can be tested. Today only few materials are considered as QSL candidates. One of them is the mineral herbertsmithite, ZnCu₃(OH)₆Cl₂ [2]. The Cu^{2+} (S = 1/2) ions in this compound form a quasi-2D layered structure with kagome lattice [3]. Such a lattice exhibits high degree of frustration which is ideal for QSL. The rhombohedral crystal lattice (ideal kagome lattice) is stabilized by the Zn ions. The mineral clinoatacamite without Zn ions, Cu₄(OH)₆Cl₂, is then monoclinic and consequently antiferromagnetic order is stabilized at low temperatures [4]. The investigation of the ground state properties in the Zn-substituted series, Zn_xCu_{4-x}(OH)₆Cl₂,

has therefore motivated numerous studies over the past two decades, usually on powder samples. In addition to their intriguing magnetic properties these compounds are also interesting from structural point of view. It is demonstrated by high amount of structural polymorphs. The presented study of single-crystalline samples is focused on the relation among these polymorphs and their ground-state properties, studied by low-temperature X-ray diffraction and specific heat measurements.

- 1. L. Balents, Nature, 464, (2010), 7286.
- 2. M. R. Norman, Rev. Mod. Phys., **88**, (2016) 041002.
- S. W. Braithwaite, R., Mereiter, K., Paar, W., Clark, A., Mineral. Mag., 68, (2004), 527-539.
- S.-H. Lee, H. Kikuchi, Y. Qiu, B. Lake, Q. Huang, K. Habicht, K. Kiefer, Nat. Mater., 6, (2007), 853-857.

This work was supported by the Czech Science Foundation via research project GAČR 23-06810O.



DIFFUSE SCATTERING IN (K,Na)NbO₃ SOLID SOLUTIONS

J. E. Flores Gonzales^{1,2}, N. Zhang³, Z. An³, M. Paściak¹

¹FZU - Institute of Physics of the Czech Academy of Sciences, Czech Republic ²Faculty of Mathematics and Physics, Charles University, Czech Republic ³Electronic Materials Research Laboratory, Key Laboratory of the Ministry of Education & International Center for Dielectric Research, School of Electronic Science and Engineering, Xi'an Jiaotong University, Xi'an, China.

floresgon@fzu.cz

In KNbO₃, the spontaneous polarization originates from displacements of Nb ions relative to the surrounding oxygen octahedra. In the rhombohedral phase, all Nb displacements are aligned along the same [111] direction, whereas in higher-symmetry phases this alignment becomes progressively less restricted due to a stepwise increase in the number of allowed Nb-displacement directions along 111. The orthorhombic phase allows two equivalent directions, the tetragonal phase four, and the cubic phase eight. This progressive increase in allowed displacement orientations introduces correlated disorder manifested by the stepwise appearance of diffuse scattering sheets in reciprocal space, evolving from (010) in the rhombohedral phase, to (010) and (100) in the tetragonal phase, and finally to {001} in the cubic phase [1].

(K,Na)NbO₃ solid solutions (KNN) are one of the leading Pb-free substitutes for (Pb,Zr)TiO₃ (PZT) with tunable piezoelectric coefficients [2]. Studies show the existence of a polymorphic phase boundary that might lead to extremely increased piezoelectric coefficients [3]. While it is accepted that the chemical disorder has a decisive role in pro-

ducing this enhanced behavior, the exact short-range structure-property mechanisms are not well understood.

In this work we are interested in how addition of $NaNbO_3$ is affecting the correlation structure across the phase transitions. In particular, it is known that pure sodium niobate displays a complex behavior with at least six phase transitions between the high-temperature cubic phase and low-temperature rhombohedral one [4]. Some of the intermediate phases are incommensurate reflecting a complex interplay between polar order parameter and octahedral tilting. Tracking the changes in the single-crystal diffuse scattering we should be able to assess to which extent this interplay is also present in KNN with Na content 50 %.

- R. Comes, M. Lambert, and A. Guinier, Solid State Commun. 6, 715 (1968).
- X. Gao, Z. Cheng, Z. Chen, et al., Nat. Commun. 12, 881 (2021).
- 3. J. Fu and R. Zuo, Acta Mater. 195, 446 (2020).
- 4. E. Ringgaard and T. Wurlitzer, J. Eur. Ceram. Soc. 25, 2701 (2005).